Hypervelocity stars from young stellar clusters in the Galactic Centre

G. Fragione,[1][*] R. Capuzzo-Dolcetta[1] and P. Kroupa[2,3]

[1]*Department of Physics, Sapienza, University of Rome, P.le A. Moro 2, I-00185 Roma, Italy*
[2]*Helmholtz-Institut für Strahlen-und Kernphysik, Universität Bonn, Nussallee 14-16, D-53115 Bonn, Germany*
[3]*Charles University in Prague, Faculty of Mathematics and Physics, Astronomical Institute, V Holešovičkách 2, CZ-180 00 Praha 8, Czech Republic*

ABSTRACT

The enormous velocities of the so-called hypervelocity stars (HVSs) derive, likely, from close interactions with massive black holes, binary stars encounters or supernova explosions. In this paper, we investigate the origin of HVSs as consequence of the close interaction between the Milky Way central massive black hole and a passing-by young stellar cluster. We found that both single and binary HVSs may be generated in a burst-like event, as the cluster passes near the orbital pericentre. High-velocity stars will move close to the initial cluster orbital plane and in the direction of the cluster orbital motion at the pericentre. The binary fraction of these HVS jets depends on the primordial binary fraction in the young cluster. The level of initial mass segregation determines the value of the average mass of the ejected stars. Some binary stars will merge, continuing their travel across and out of the Galaxy as blue stragglers.

Key words: stars: kinematics and dynamics – Galaxy: centre – Galaxy: kinematics and dynamics – galaxies: star clusters: general.

1 INTRODUCTION

Hypervelocity stars (HVSs) are stars escaping the Milky Way (MW) gravitational well. Whereas Hills (1988) predicted theoretically their existence, HVSs were observed for the first time only 17 yr later by Brown et al. (2005). About 20 HVSs have been found at velocities up to $\approx 700 \, \mathrm{km \, s^{-1}}$ in the outer MW halo (between 50 and 120 kpc) by the Multiple Mirror Telescope (MMT) spectroscopic survey (Brown et al. 2010; Brown, Geller & Kenyon 2014). This survey targets stars with magnitudes and colours typical of 2.5–4 $\mathrm{M_\odot}$ late B-type stars. As consequence of the target strategy, the MMT stars could be either main-sequence B stars, evolved blue horizontal branch stars or blue stragglers (Brown et al. 2014). Recently, astronomers have started to investigate low-mass HVS candidates (Li et al. 2015; Ziegerer et al. 2015). Being a MMT spectroscopic survey, HVS data suffer from the lack of tangential velocity measurements. The astrometric European satellite *Gaia* (http://www.cosmos.esa.int/web/gaia) is expected to measure proper motions with an unprecedented precision, providing a larger and less biased sample of HVSs (allegedly ≈ 100 in a catalogue of $\approx 10^9$ stars). Moreover, *Gaia*'s sensitivity is good enough to search for multiplanet systems around massive stars and to reveal their architectures and three-dimensional orbits, giving the possibility of spotting some planetary transits around HVSs (Ginsburg, Loeb & Wegner 2012; Fragione & Ginsburg 2017).

The Hills mechanism (Hills 1988) involves the tidal breakup of a binary that passes close to the MW black hole (BH) (Ginsburg & Loeb 2006, 2007; Löckmann, Baumgardt &

Kroupa 2008; O'Leary & Loeb 2008; Sari, Kobayashi & Rossi 2009), but the physical mechanism responsible for the production of the observed HVSs is still debated. Other possible origins have been advanced (Brown 2015), such as the interaction of a BH binary with a single star (Yu & Tremaine 2003), the interaction of star clusters and BHs (Capuzzo-Dolcetta & Fragione 2015; Fragione & Capuzzo-Dolcetta 2016), supernova explosions (Zubovas, Wynn & Gualandris 2013; Tauris 2015), tidal disruption of a dwarf galaxy passing through the Galactic Centre (GC) (Abadi, Navarro & Steinmetz 2009) and the dynamical evolution of a thin and eccentric disc orbiting around a massive BH (Šubr & Haas 2014, 2016; Haas & Šubr 2016). The extreme velocities of HVSs indicate they may derive from a strong dynamical interaction with BHs in the GC or in a nearby galaxy (Sherwin, Loeb & O'Leary 2008).

The importance of HVSs is that they can provide information on the environment where they were born (Gould & Quillen 2003). In particular, they can discriminate between a single and a binary BH in the GC (Sesana, Haardt & Madau 2007). Since their orbits are determined by the MW potential, HVS kinematics can be used to probe the Galactic potential's triaxiality (Gnedin et al. 2005; Yu & Madau 2007) and discriminate among different Galactic mass distributions (Perets et al. 2009; Gnedin et al. 2010; Fragione & Loeb 2016).

As Capuzzo-Dolcetta & Fragione (2015) and Fragione & Capuzzo-Dolcetta (2016) have shown, a relevant mechanism to accelerate stars to high or even hypervelocities is that due to the close interaction of a single or binary massive BH and a passing-by massive stellar cluster (Arca-Sedda, Capuzzo-Dolcetta & Spera 2016). In the cited works, the analysis was done for an evolved globular cluster-like object. The aim of this paper is, instead, that of investigating a possible origin of HVSs that involves a Young Star

[*] E-mail: giacomo.fragione@uniroma1.it

Cluster (YSC) that, during its orbit, has had the chance to pass close to the MW central supermassive black hole (SMBH). When the YSC passes by the SMBH, some of its stars can be stripped from the cluster and ejected with high velocities (Capuzzo-Dolcetta & Fragione 2015; Fragione & Capuzzo-Dolcetta 2016).

The outline of the paper is as follows. In Section 2, we describe the method we use to study the consequences of YSC–BH interaction. In Section 3, the results are presented and discussed. Finally, in Section 4, we summarize our main conclusions.

2 METHOD

We use the publicly available code MCLUSTER to generate initial conditions for the YSC (Küpper et al. 2011). MCLUSTER sets up initial conditions once the desired features of the cluster are specified, such as the total mass M_{cl} (or alternatively the total number of stars N), the density profile, the initial degree of mass segregation S and the primordial binary fraction B.

We studied a YSC interacting with the SgrA* SMBH via direct N-body simulations. To do this, we consider a set of six cluster models, which differ in the initial binary fraction (B) and in the initial degree of mass segregation (S). B is defined as

$$B = \frac{N_b}{N_b + N_s}, \tag{1}$$

where N_b is the number of binaries and N_s is the number of single stars in the cluster. The initial binary fraction of our models assumes the values $B = 0, 0.25, 0.5, 0.75, 1$ for both segregated ($S = 1$) and unsegregated ($S = 0$) clusters. Note that some of our models have a high initial binary fraction. Such an assumption is justified by the fact that both theory and observations suggest that the angular momentum of a collapsing cloud core may be distributed more efficiently into two stars (Goodwin & Kroupa 2005; Marks & Kroupa 2012; Leigh et al. 2015; Oh, Kroupa & Pflamm-Altenburg 2015) rather than into a single star or a higher order multipole system. Initially mass-segregated clusters are generated with the method developed in Baumgardt, De Marchi & Kroupa (2008). In a few words: if the cluster is completely mass segregated ($S = 1$), MCLUSTER assigns the lowest energy orbit to the highest mass star and the highest energy orbit to the lowest mass star. Intermediate degrees of mass segregation can be achieved by non-perfect ordering of masses and energy orbits (Küpper et al. 2011). Table 1 resumes the cases considered.

To generate initial conditions, we follow the prescriptions of Oh et al. (2015). We set the mass of the cluster to $M_{cl} = 10^3$ M$_\odot$. We note here that 10^4 M$_\odot$ clusters are observed more easily than lighter ones due to an observational bias. Star formation in the inner region of the Galaxy is likely to be producing many more low-mass clusters, which are hardly observable given the dust absorption in the whole inner Galactic region. This is why we are studying a, likely, common very young cluster, to understand whether such a

Table 1. Cluster models: name, initial binary fraction (B) and initial mass segregation fraction (S).

Name	B	S
B1S1	1	1
B1S0	1	0
B0S1	0	1
B025S1	0.25	1
B05S1	0.5	1
B075S1	0.75	1

cluster may lead to an anisotropic flux of HVSs. The cluster density distribution is modelled with a Plummer (1911) profile whose initial half-mass radius is derived from the Marks & Kroupa (2012) relation

$$r_h = 0.1 \times (M_{cl}/M_\odot)^{0.13} \text{ pc} = 0.25 \text{ pc}. \tag{2}$$

The stellar masses, m (M$_\odot$), are sampled from the initial mass function (IMF) by Kroupa (2001) and Kroupa et al. (2013):

$$\xi(m) = \begin{cases} k_1 \left(\frac{m}{0.08}\right)^{-1.3} & m_{min} \leq m/M_\odot \leq 0.50, \\ k_2 \left(\frac{0.5}{0.08}\right)^{-1.3} \left(\frac{m}{0.5}\right)^{-2.3} & 0.50 \leq m/M_\odot \leq m_{max}, \end{cases} \tag{3}$$

where $k_1 \approx 0.113$ and $k_2 \approx 0.035$ are normalization factors, $m_{min} = 0.08$ M$_\odot$ and $m_{max} = 40.54$ M$_\odot$ is chosen from the maximum stellar mass–cluster mass relation given in Weidner & Kroupa (2004) and Pflamm-Altenburg, Weidner & Kroupa (2007).

The canonical Kroupa (1995b) period distribution function is adopted for all binaries in the cluster

$$f(\log_{10} P) = 2.5 \frac{\log_{10} P - 1}{45 + (\log_{10} P - 1)^2}, \tag{4}$$

where the period, P, is in days. Stars with mass $m < 5$ M$_\odot$ are randomly paired after sampling the two masses from the chosen IMF (Kroupa 1995a,b). However, observations show that massive binaries preferentially favour massive companions (Sana et al. 2012), therefore, stars with $m \geq 5$ M$_\odot$ are paired together to follow this observational feature; for details see Oh et al. (2015). The initial binary eccentricities, e, are drawn from a thermal distribution (Kroupa 2008),

$$f_e(e) = 2e. \tag{5}$$

All the models are generated under the assumption that the clusters are in virial equilibrium (Oh et al. 2015). The time integration of the stellar system was done by means of the publicly available code NBODY6 (Aarseth 2003). Initially, the cluster centre of mass is set in the Galactic disc on the x-axis at 100 pc from the GC, with an initial velocity of 2 km s^{-1} along the Galactic y-axis (the pericentre results to be ≈ 0.45 pc and the orbital eccentricity $e_{cl} \approx 0.99$). The choice of a highly eccentric orbit is justified by our interest to study the maximum possible effect in the massive BH–YSC interaction that depends mainly on the distance of closest approach (for given values of other parameters). The role of changing the eccentricity, and so changing the pericentric distance, has been already investigated in Capuzzo-Dolcetta & Fragione (2015) and Fragione & Capuzzo-Dolcetta (2016). In particular, Capuzzo-Dolcetta & Fragione (2015) showed that the larger the eccentricity the more efficient the ejection of high-velocity stars. This effect combines with the total mass of the cluster, where a more massive cluster generates a larger fraction of fast-moving stars (as also discussed in Section 3.1).

We produced 150 different realizations of each model (generated with different random seeds) to obtain statistically relevant results.

2.1 The Milky Way potential

We describe the MW potential with a 4-component model $\Phi(r) = \Phi_{BH} + \Phi_b(r) + \Phi_d(r) + \Phi_h(r)$ (Kenyon et al. 2008, 2014; Fragione & Loeb 2016), where

(i) Φ_{BH} is the contribution of the central SMBH,

$$\Phi_{BH}(r) = -\frac{GM_{BH}}{r}, \tag{6}$$

with mass $M_{BH} = 4 \times 10^6$ M$_\odot$;

(ii) Φ_b is the contribution of the spherical bulge (Hernquist 1990),

$$\Phi_b(r) = -\frac{GM_{bul}}{r + a}, \tag{7}$$

with mass $M_b = 3.76 \times 10^9$ M$_\odot$ and core radius $a = 0.10$ kpc;

(iii) Φ_d accounts for the axisymmetric disc (Miyamoto & Nagai 1975),

$$\Phi_{disc}(R, z) = -\frac{GM_{disc}}{\sqrt{(R^2 + (b + \sqrt{c^2 + z^2})^2)}}, \tag{8}$$

with mass $M_{disc} = 5.36 \times 10^{10}$ M$_\odot$, length scale $b = 2.75$ kpc and scale height $c = 0.30$ kpc;

(iv) Φ_{halo} is the contribution of the dark matter halo (Navarro, Frenk & White 1997)

$$\Phi_{halo}(r) = -\frac{GM_{DM} \ln(1 + r/r_s)}{r}, \tag{9}$$

with $M_{DM} = 10^{12}$ M$_\odot$ and length scale $r_s = 20$ kpc.

The parameters are chosen so that the Galactic circular velocity at the distance of the Sun (8.15 kpc) is 235 km s^{-1} (Reid et al. 2014).

3 RESULTS

In our simulations the fate of the stars in the cluster is determined by their final amount of energy. After the close cluster–BH interaction a star can remain bound to the cluster (Arca-Sedda et al. 2016), or can be captured by the BH (Gould & Quillen 2003; Ginsburg & Loeb 2006; Perets, Hopman & Alexander 2007) or can be lost from the system (Capuzzo-Dolcetta & Fragione 2015; Fragione & Capuzzo-Dolcetta 2016). In this paper, we focus our attention on the stars lost by the system and ejected at such velocities to become unbound with respect to the Galaxy, examining, in this context, the role of the cluster initial binary fraction and mass segregation. Fig. 1 shows snapshots at different times of the cluster model B1S1, and the production of single and binary HVSs after the close interaction with the BH.
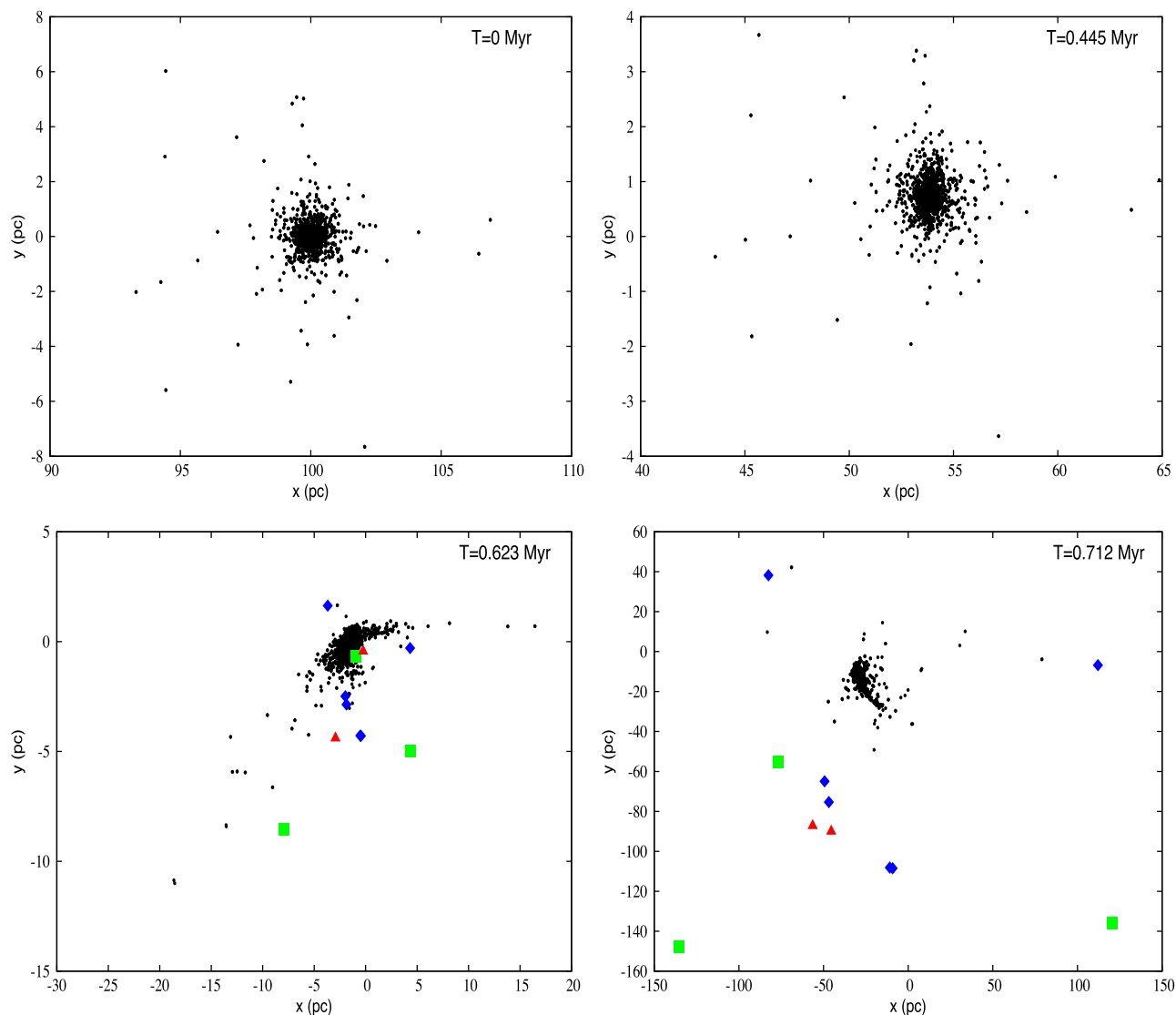

Figure 1. Snapshots at different times of the cluster model B1S1. After the pericentre passage, single and binary HVSs are produced. In the bottom panels, green squares represent binary HVSs, red triangles represent single HVS produced via the first two mechanisms described in Section 3, blue diamonds represent HVSs produced via the third mechanism described in Section 3. The massive BH has coordinates $(x, y, z) = (0, 0, 0)$.
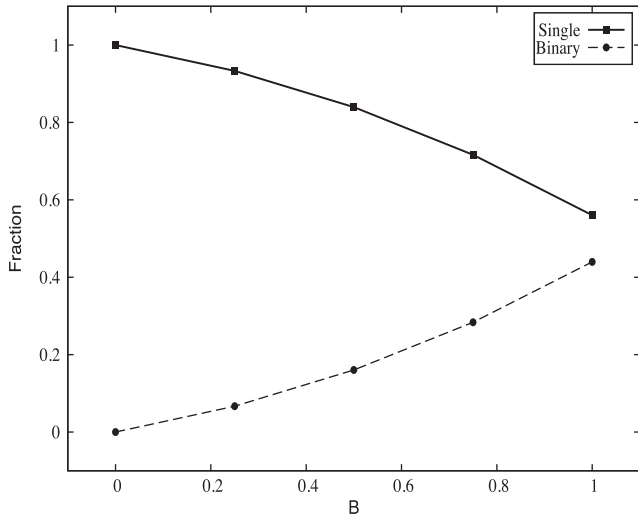
Figure 2. Fraction of single ($N_{s,HVS}/N_{HVS}$) and binary ($N_{b,HVS}/N_{HVS}$) HVSs as function of the cluster binarity.

The relative (to the total) number of ejected (single and binary) HVSs depends on the initial content of binaries (see Fig. 2). As B increases, the number of ejected binary HVSs, $N_{b,HVS}$, increases. On the other hand, the relative fraction $N_{s,HVS}/N_{HVS}$, where $N_{s,HVS}$ and $N_{HVS} = N_{s,HVS} + N_{b,HVS}$ are the number of single HVSs and the total number of HVS systems, respectively, of ejected single HVSs decreases as the initial content of binaries in the cluster is larger.

We find three possible sources of single HVSs. The first mechanism is equivalent to Hills' binary disruption (Hills 1988). In this process, HVS is generated as a consequence of the disruption of a binary star that undergoes a close interaction with the Galactic SMBH. In this case, one of the two stars is captured by the SMBH and becomes an S-star (Gould & Quillen 2003; Perets et al. 2007; Löckmann et al. 2008). The second production channel involves a single star and the other $N - 1$ stars of the cluster. During the close passage of the cluster around the SMBH, a single star may be removed from the cluster due to the coupled YSC+BH gravitational interaction (Capuzzo-Dolcetta & Fragione 2015; Fragione & Capuzzo-Dolcetta 2016). The third mechanism is the splitting of a binary HVS into two single HVSs. Whereas single HVSs can originate from three different mechanisms, binary HVSs can originate only from the previous process. Actually, after the ejection from the cluster the binary can undergo three different fates. One possibility is that the binary star survives, travelling farther at hypervelocity. If the binary does not survive, it can either merge or disrupt as a consequence of the velocity kick due to the interaction with the SMBH, splitting into two single HVSs. This is, actually, the third channel for producing single HVSs. When the binary is accelerated, the kick velocity has to be combined with the binary orbital velocity. For simplicity, let us consider the case where the kick velocity vector is coplanar with the orbital velocity vector of the stars. It may happen that at the moment of the ejection the velocity of one of the stars in the pair is nearly aligned with the kick, while the companion velocity is unaligned. In this case, the orbital velocity of the former enhances the kick velocity, while the latter has a slightly lower ejection velocity. As a consequence, both the stars of the binary are accelerated to hypervelocities, but start to diverge from each other.

Figs 3 and 4 show the resulting ejection velocity distributions for the models considered. Fig. 3 illustrates the resulting velocity distributions of single HVSs for different initial binary fractions of the YSC. We included in the distribution all the stars with velocity beyond the local escape speed $v_{es}(r)$, as determined by the Galactic model (see Section 2.1), and consider their velocity at the reference distance of 1 pc from the central BH. The local (at 1 pc) escape speed is $v_{es} \approx 940 \, \mathrm{km \, s^{-1}}$, which corresponds to the cutoff in the plots. The distributions extend up to ≈ 4000–$5000 \, \mathrm{km \, s^{-1}}$. We fitted our data with four different functions, i.e. the gamma, Weibull, lognormal and normal functions. The Kolmogorov–Smirnov statistical test favours the normal distribution. Fig. 4 shows the velocity distributions of single and binary HVSs for the model B1S1, along with the same fits of Fig. 3. Also in this case, the best fit is given by the normal distribution.

Capuzzo-Dolcetta & Fragione (2015) demonstrated that another important feature of the high-velocity stars originated as a consequence of the interaction of a globular cluster and a massive BH is the significant level of collimation of the ejected stars. As an illustrative example, Fig. 5 shows the distributions of the Galactocentric latitude and longitude of single HVSs for the model B1S1. As mentioned above, the cluster centre of mass is set on the Galactic x-axis at 100 pc off the MW centre and has an initial velocity $2 \, \mathrm{km \, s^{-1}}$ along the Galactic positive y-axis. As a consequence of the chosen initial conditions, the cluster centre-of-mass orbital motion lies in the Galactic disc. Fig. 5 (top panel) shows that initially the latitude distribution is peaked at $0°$. This result means that the HVSs are ejected nearly in the initial cluster orbital plane. On the other hand, the longitude distribution of HVSs quantifies the ejection direction with respect to the orbital motion of the cluster. Capuzzo-Dolcetta & Fragione (2015) demonstrated that high-velocity stars are collimated and preferentially ejected near the cluster pericentre. Fig. 5 (bottom panel) shows the resulting longitude distribution. The distribution presents a peak at $\approx 190°$, while the cluster centre-of-mass velocity at pericentre has $\theta = 180°$. This indicates that HVSs are ejected near the pericentre along the direction of motion of the cluster.

Our results suggest that this mechanism produces single and binary HVSs in burst-like events (when the cluster is near pericentre), which will move on the orbital plane and in the direction of the cluster orbital motion. Moreover, the binary fraction of these HVS 'jets' depends on the initial binary fraction in the progenitor cluster.

We investigated also the role of the initial mass segregation comparing results of model B1S1, fully mass segregated, with those of model B1S0, not mass segregated. We see that the segregation affects the mass distribution of HVSs. Fig. 6 shows the mass distribution of the ejected single HVSs for the cases under consideration. For the case of the fully segregated YSC, ≈ 97 per cent of ejected HVSs have $m_* \lesssim 0.5 \, \mathrm{M_\odot}$. Whereas, for an unsegregated YSC, the amount of stars with $m_* \gtrsim 0.5 \, \mathrm{M_\odot}$ is not negligible (≈ 20 per cent of all HVSs). It is interesting to note that our model predicts the production of low-mass HVSs, as a consequence of the fact that the initial average stellar mass in the YSC is $\approx 0.5 \, \mathrm{M_\odot}$. However, the observed HVSs are probably main-sequence B stars with $m_* \approx 3$–$4 \, \mathrm{M_\odot}$ (Brown et al. 2014). Hence, if HVSs originated from the infall of a YSC, the initial mass segregation fraction had to be $S \approx 0$. Brown, Geller & Kenyon (2008) showed that HVSs are clustered in the direction of the constellation Leo (see also Brown et al. 2014). Brown, Geller & Kenyon (2012) suggested that the HVSs anisotropy may reflect the anisotropy of the MW gravitational potential. In the Šubr & Haas (2016) model, the anisotropy reflects the disc inclination from which HVSs are generated. In our model, the anisotropy of HVSs is a natural consequence of the cluster motion at the pericentre, while the flight times of the HVSs clumped around
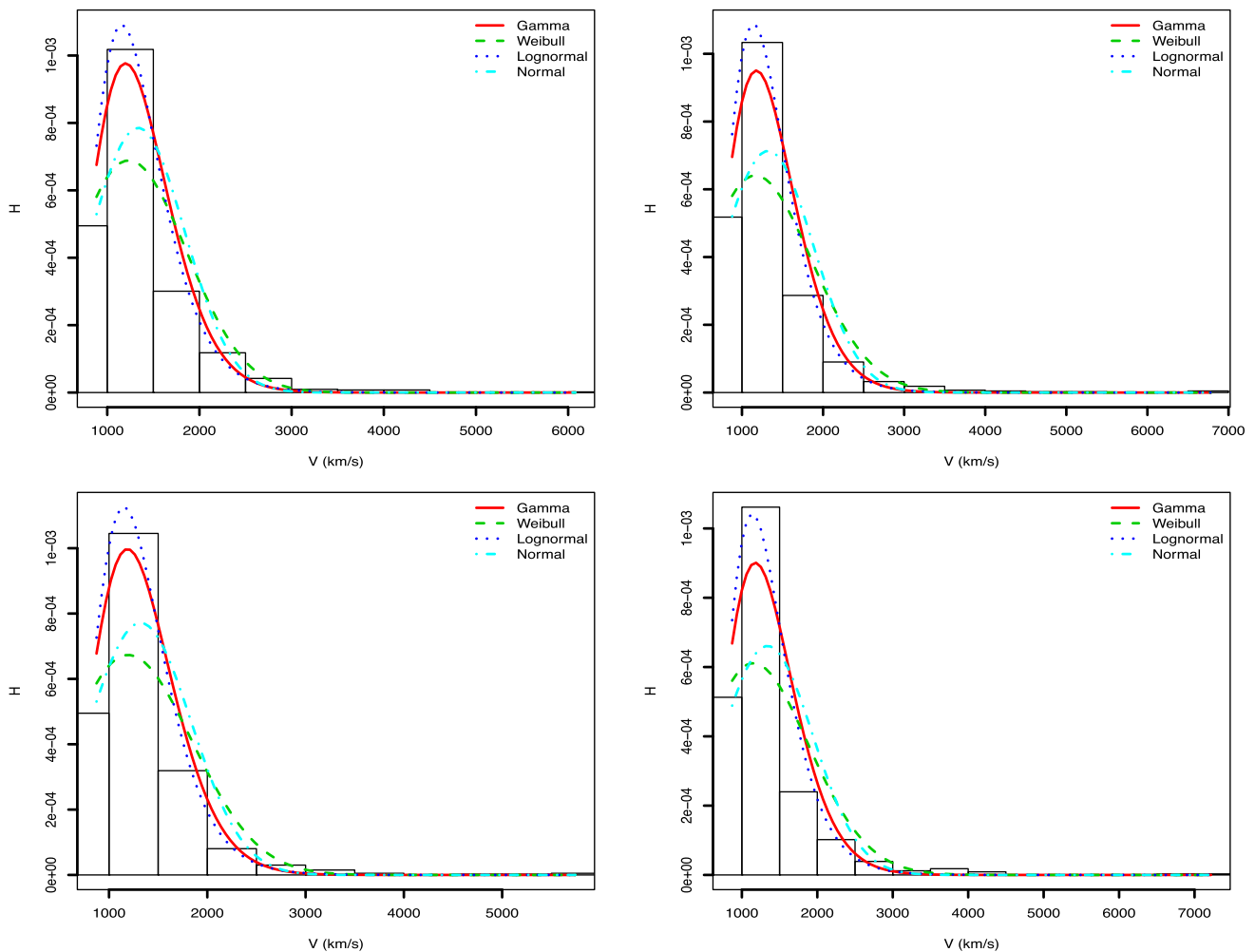
Figure 3. Distribution function of the velocity of single HVSs in models B0S1 (top-left), B025S1 (top-right), B05S1 (bottom-left) and B075S1 (bottom-right). Here H is normalized to area of 1.

the constellation Leo can be described by successive bursts of HVSs produced by successive interactions between the cluster and the BH.

3.1 The effect of a top-heavy IMF

De Marchi, Paresce & Pulone (2007) showed for the first time that clusters depleted in low-mass stars have a low concentration, which is incompatible with a canonical Kroupa (2001) IMF modelled by standard secular two-body relaxation evolution (Leigh et al. 2012). Marks, Kroupa & Baumgardt (2008) proposed a residual-gas expulsion scenario to solve this inconsistency (Marks & Kroupa 2010). In this scenario, the quick gas removal from compact and primordially mass-segregated clusters leads to low-concentration clusters that are depleted in low-mass stars. Concerning stars with masses $\gtrsim 1\,M_\odot$, their content depends on the ambient star-forming conditions. Elmegreen & Shadmehri (2003) demonstrated that densely packed stars would produce top-heavy IMFs in the most massive and dense clusters. It may be difficult to observe evidence for a top-heavy IMF, since stars with mass $\gtrsim 1\,M_\odot$ have evolved away from the main sequence in those globular clusters, where a primordial top-heavy IMF is expected to be found (Marks et al. 2012). However, some YSCs show evidence of a primordial top-heavy

IMF, such as the Arches cluster (located about 25 pc in projected distance from the GC). A top-heavy IMF can be described by

$$\xi(m) = \begin{cases} h_1 \left(\frac{m}{0.08}\right)^{-1.3} & m_{min} \le m/M_\odot \le 0.50, \\ h_2 \left(\frac{m}{0.5}\right)^{-2.3} & 0.50 \le m/M_\odot \le 1.0, \\ h_3 \left(\frac{m}{1.0}\right)^{-\alpha_3} & 1.0 \le m/M_\odot \le m_{max}, \end{cases} \quad (10)$$

where h_1, h_2 and h_3 are normalization factors [such that $\xi(m)$ is a continuous function] and α_3 measures the steepness of the top-heavy IMF. Observations show that $1.65 \le \alpha_3 \le 2.3$ for the Arches cluster (Marks et al. 2012).

In this section, we show the effects of a top-heavy IMF on the originated HVSs. We compare the results for the model B0S1 with the same model, in which the masses of the stars are sampled from a top-heavy IMF, i.e. for the same cluster mass an IMF with more massive stars than expected from the canonical (Kroupa 2001) IMF.

In our simulations, we use equation (10) with $\alpha_3 = 1.65$ to sample stellar masses. We find that the presence of a primordial top-heavy IMF influences the average mass of the produced HVSs. Fig. 7 shows the mass distribution of the ejected HVSs for the cases under consideration. As discussed above, while for the case of a canonical IMF ≈ 97 per cent of the ejected HVSs have $m_* \lesssim 0.5\,M_\odot$ (top panel), the amount of stars with $m_* \gtrsim 0.5\,M_\odot$ is not negligible
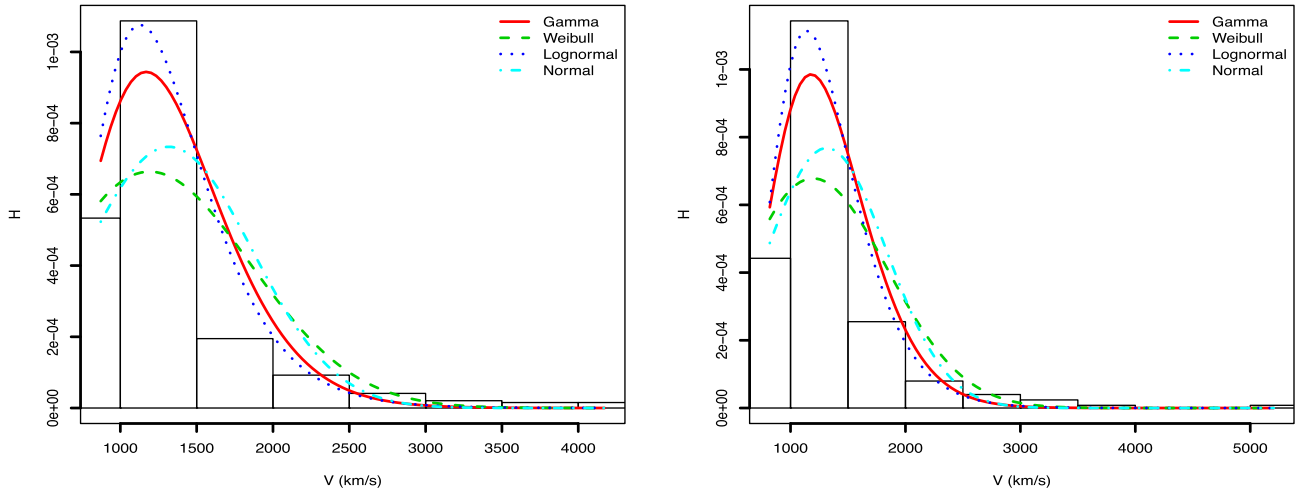
Figure 4. Distribution function of the velocity of single (left) and binary (right) HVSs for the model B1S1.
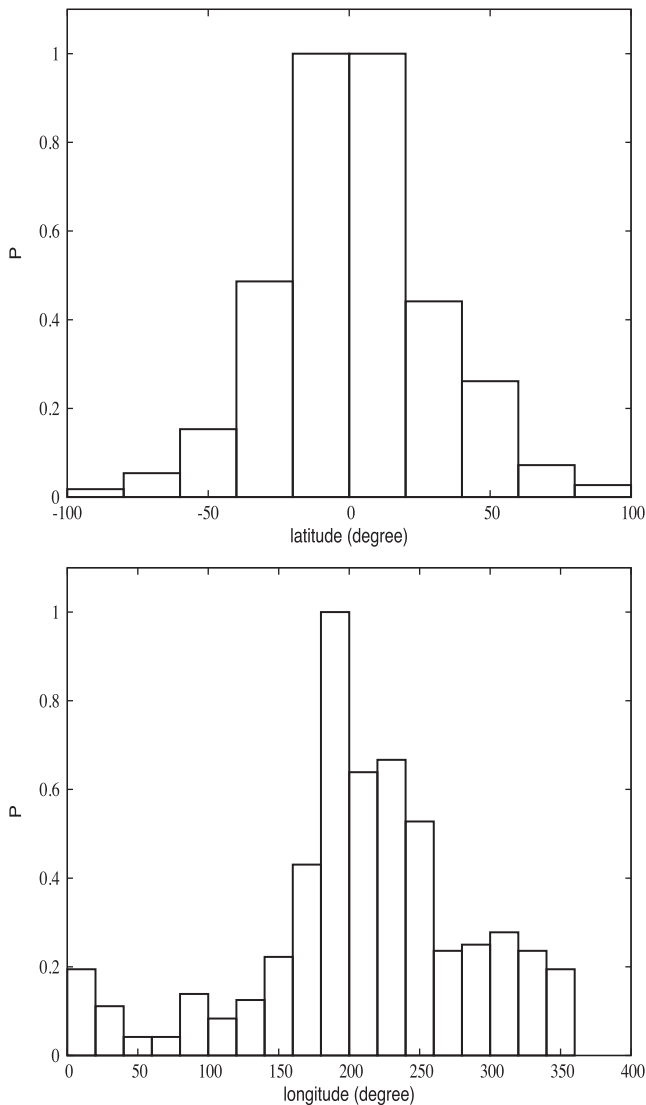

Figure 5. Latitude and longitude of single HVSs for the model B1S1. Here P is normalized to the maximum value.

($\approx$18 per cent of all HVSs) when considering a top-heavy IMF (central panel). Fig. 7 illustrates also the mass distribution of the ejected HVSs for the case $M_{cl} = 10^4 \, M_\odot$. In this case, $r_h = 0.33 \, pc$ (Marks & Kroupa 2012) and $m_{max} \approx 110.42 \, M_\odot$ in equation (3) (Weidner & Kroupa 2004; Pflamm-Altenburg et al. 2007). Fig. 7 shows that the amount of stars with $m_* \gtrsim 0.5 \, M_\odot$ is not negligible ($\approx$15 per cent of all HVSs) when considering a $M_{cl} = 10^4 \, M_\odot$ cluster (bottom panel). Fig. 7 also illustrates that the maximum mass of the ejected HVSs increases when dealing with more massive clusters, as a consequence of the Weidner & Kroupa (2004) relation used for m_{max} (we found HVSs with masses up to $\approx$15 $M_\odot$). The effect of a top-heavy IMF and of a more massive cluster is comparable to the one induced by primordial mass segregation concerning the average mass of ejected HVSs. As shown, initially not segregated clusters lead to a not negligible fraction of massive HVSs. If some of the observed HVSs originated from the infall of a YSC, three possible explanations are feasible, i.e. the cluster initial mass segregation $S \approx 0$, or the cluster primordial IMF was top-heavy, or $M_{cl} \gtrsim 10^4 \, M_\odot$. Moreover, the efficiency in converting cluster stars into HVSs is about one order of magnitude larger with respect to the $10^3 \, M_\odot$ cluster (see also Capuzzo-Dolcetta & Fragione 2015).

Concerning the Arches cluster, Harfst, Portegies Zwart & Stolte (2010) showed that, upon comparison of simulations with observations, it may be described by a King (1966) model with a value of the central dimensionless potential $W_0 = 3$. We perform simulations for the model B0S1, whose star distribution is sampled from a King (1966) profile with $W_0 = 3$. Fig. 8 shows the distribution function of the velocity of the produced HVSs and their masses. We find that there are no significant differences from the case where stars are sampled from a Plummer (1911) profile. We note here that the Plummer density distribution function is the simplest solution to the collisionless Boltzmann equation, that it well describes the simplest stellar dynamical systems (Plummer 1911) and that it evolves to a King profile due to the energy equipartition process and the influence of the tidal field.

3.2 The fate of hypervelocity binary stars

We study the fate of the ejected binary HVSs. As discussed, binary HVSs can undergo three different fates. The binary star can survive
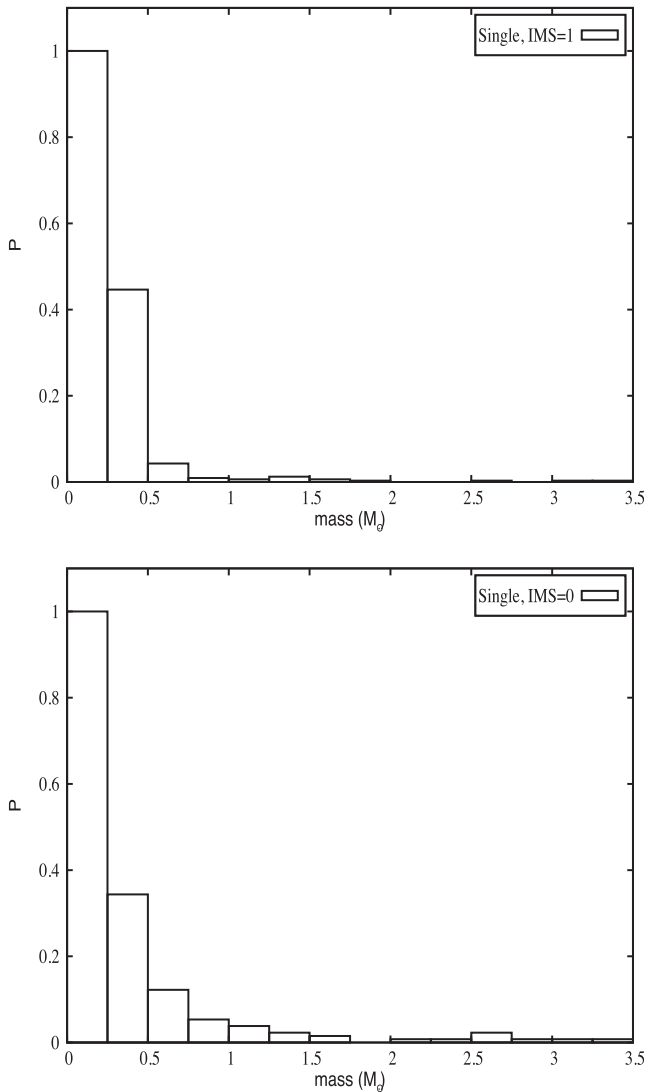
Figure 6. Masses of HVSs with (top, model B1S1) and without initial mass segregation (bottom, model B1S0).

travelling farther at hypervelocity, can merge or can be disrupted as a consequence of the velocity kick.

Fig. 9 shows the fraction of single HVSs that originates as consequence of the binary disruption discussed in the previous section. This fraction increases when the initial binary fraction is larger. For the case $B = 1$ about 60 per cent of single HVSs are generated through this channel.

Fig. 10 shows the mass, eccentricity and semimajor axis of binary HVSs for the model B1S1. Due to the initial choice of mass sampling from the canonical IMF (Kroupa 2001; Kroupa et al. 2013), the mass distribution (top panel) is peaked at $m_* \lesssim 0.5\,\mathrm{M_\odot}$. The eccentricity distribution (central panel) shows that ejected binaries are highly eccentric, with a peak at $e \approx 0.7$. The semimajor axis distribution (bottom panel) indicates that most of the ejected binary HVSs have $a \lesssim 100$ au. Because the average stellar mass in the YSC is ≈ 0.5, the total mass of the binary $\approx 1\,\mathrm{M_\odot}$ and $P \propto a^{3/2}$, the period of binary HVSs results to be $P \lesssim 10^3$ d. Fig. 10 thus indicates, so, that the binary HVSs ejected from an infalling YSC are generally compact and eccentric.

Such eccentric and compact binary stars can merge while travelling across the Galaxy at hypervelocities. If we assume that the
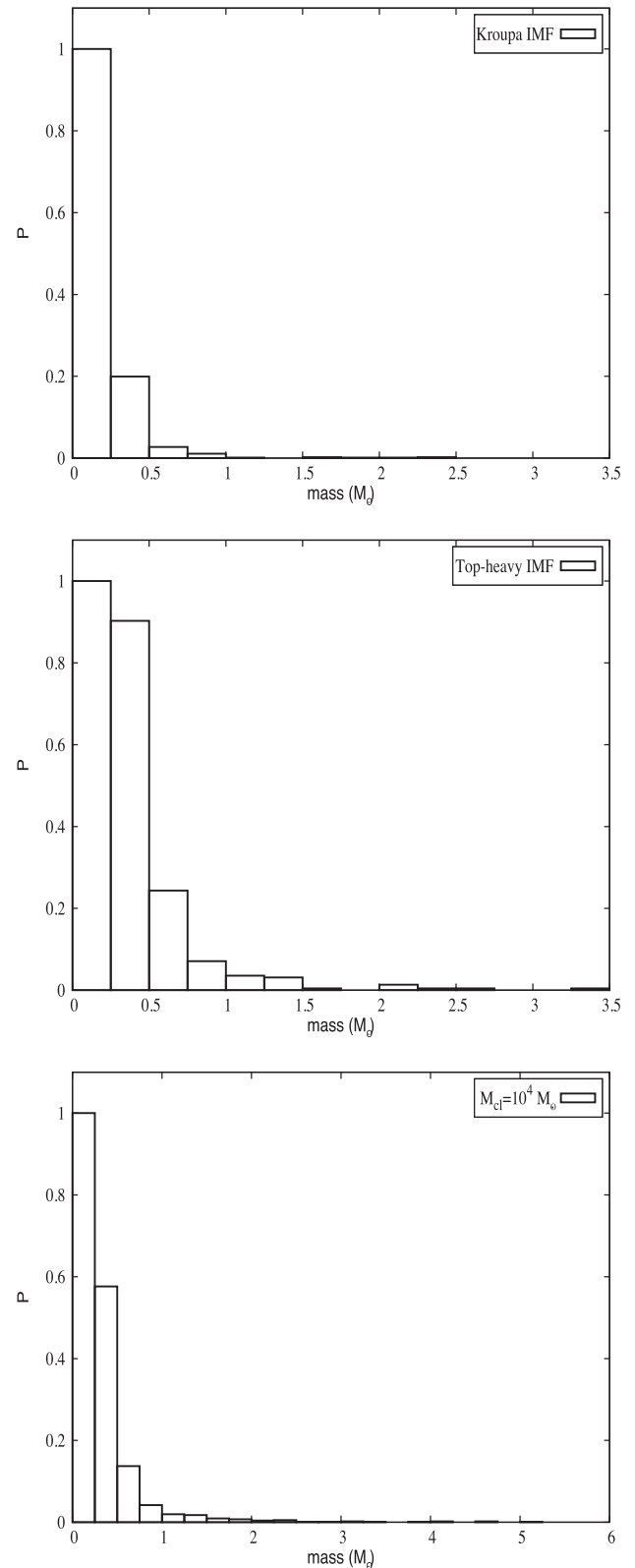

Figure 7. Masses of HVSs with canonical Kroupa IMF (top, model B0S1) and top-heavy IMF (centre, model B0S1) for the case $M_{cl} = 10^3\,\mathrm{M_\odot}$ and masses of HVSs with canonical Kroupa IMF (bottom, model B0S1) for the case $M_{cl} = 10^4\,\mathrm{M_\odot}$.
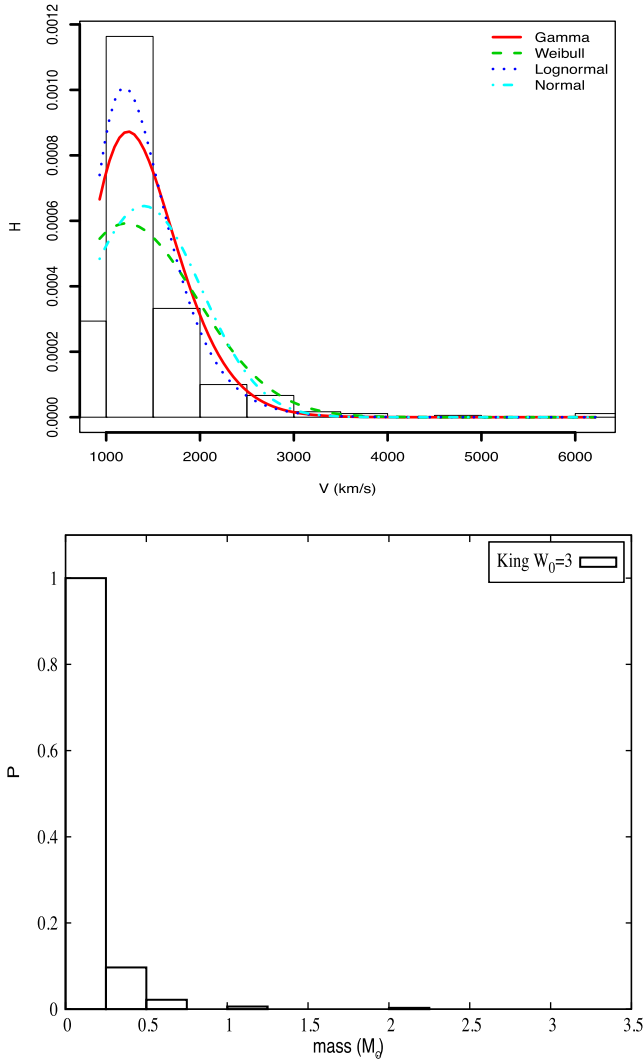
Figure 8. Distribution function of the velocity of HVSs (top) and their masses (bottom) for the model B0S1 for the case the cluster density profile is modelled with a King (1966) profile with $W_0 = 3$ and $r_h = 0.25$ pc. There is no statistically significant difference to the Plummer case [Fig. 3 (top-left panel) and Fig. 7 (top panel).]

evolution of a binary is described by the Kroupa (1995b) eigenevolution, the evolution of orbital elements occurs when the stars of the binary are at the pericentre

$$R_{\mathrm{per}} = (1-e) \left(\frac{P_b}{1\,\mathrm{d}} \right)^{2/3} \left(\frac{m_1 + m_2}{1\,\mathrm{M}_\odot} \right)^{1/3} \,\mathrm{au}, \qquad (11)$$

where e is the binary eccentricity, P_b is the binary period in days and m_1 and m_2 are the masses of the primary and secondary, respectively. According to Kroupa (1995b), the binary eccentricity evolves, after the ejection from the cluster, according to

$$\frac{\dot{e}}{e} = -\dot{\rho}, \qquad (12)$$

where

$$\rho = \left(\frac{\lambda R_\odot}{R_{\mathrm{per}}} \right)^\chi . \qquad (13)$$

In the previous equation, $R_\odot = 4.6523 \times 10^{-3}$ au is the Sun's radius, while λ indicates the length scale over which significant evolution of the orbital elements occurs, χ measures the interaction strength
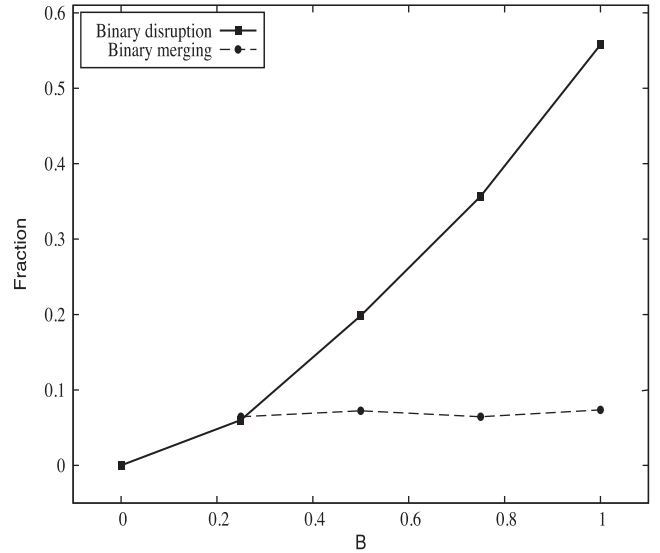

Figure 9. Disrupted and merged binary HVSs.

of the two stars (Kroupa 1995b). If eigenevolution occurs during pre-main-sequence $\lambda = 28$ and $\chi = 0.75$, whereas $\lambda_{\mathrm{ms}} = 24.7$ and $\chi_{\mathrm{ms}} = 8$ for the case of main-sequence phase. The initial binary period $P_{\mathrm{b,in}}$ evolves to

$$P_{\mathrm{b,fin}} = P_{\mathrm{b,in}} \left(\frac{m_{\mathrm{tot,in}}}{m_{\mathrm{tot,fin}}} \right)^{1/2} \left(\frac{1-e_{\mathrm{in}}}{1-e_{\mathrm{fin}}} \right)^{3/2}, \qquad (14)$$

where $m_{\mathrm{tot,in}}$ and $m_{\mathrm{tot,fin}}$ are the initial and final total mass, respectively. On the other hand, the initial mass ratio $q_{\mathrm{in}} = m_1/m_2$ is assumed to evolve to

$$q_{\mathrm{fin}} = q_{\mathrm{in}} + (1 - q_{\mathrm{in}})\rho^*, \qquad (15)$$

where

$$\rho^* = \begin{cases} \rho & \rho \leq 1, \\ 1 & \rho > 1. \end{cases} \qquad (16)$$

Finally, the final mass of the secondary will be $m_{2,\mathrm{fin}} = q_{\mathrm{fin}} m_{1,\mathrm{in}}$, while $m_{1,\mathrm{fin}} = m_{1,\mathrm{in}}$. The components of the binary are considered merged if their semimajor axis after eigenevolution is $\lesssim 10\,R_\odot$ (Kroupa 1995b).

We apply the eigenevolution to the ejected binary HVSs to quantify how many of them will merge. Fig. 9 shows the fraction of binaries that merge, as a consequence of the eigenevolution, as a function of the initial binary fraction. The same binaries merge both if we use pre-main-sequence λ, χ and main-sequence λ_{ms}, χ_{ms}, since merging binaries are very compact ($a \lesssim 0.2$ au) and eccentric ($e \gtrsim 0.7$). We find that the fraction of merged binaries is nearly constant (≈ 7 per cent) independent of the initial B. This small fraction of HVSs will continue their paths in the Galactic field as blue stragglers.

4 CONCLUSIONS

In this paper, we investigated the origin of HVSs as a consequence of the close passage of a YSC around the MW central SMBH. During the close encounter, some stars are stripped from the cluster and may be ejected with high velocities (Capuzzo-Dolcetta & Fragione 2015; Fragione & Capuzzo-Dolcetta 2016). We focused our attention on the stars lost by the system and ejected at hypervelocities after the
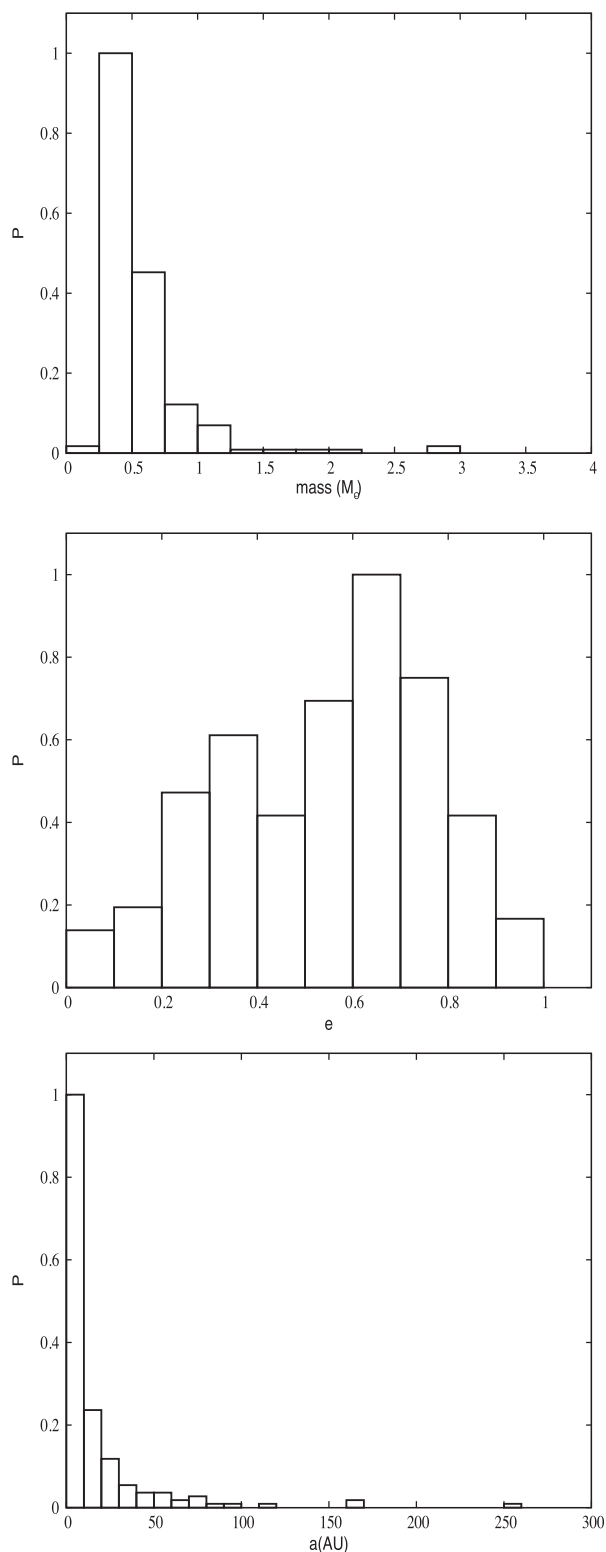
Figure 10. Mass (top), eccentricity (centre) and semimajor axis (bottom) distributions of binary HVSs for the model B1S1.

interaction with the BH, examining the role of the cluster initial binary fraction and mass segregation.

We found that this mechanism produces single and binary HVSs in a burst-like event (when the cluster is at the orbital pericentre), nearly in the initial cluster orbital plane and in the direction of

the cluster orbital motion. The binary fraction of these HVSs jets depends on the initial fraction of binaries in the progenitor cluster. On the other side, the initial mass segregation affects the mass of ejected stars: the smaller the initial segregation fraction, the larger the average mass of HVSs. Moreover, we found that also the top-heaviness of the IMF and the total mass of the cluster affects the mass distribution of HVSs: a top-heavy IMF and a large cluster mass increase the average mass of HVSs.

We also quantified how many binary stars survive at hyper-velocities. Applying the Kroupa (1995b) eigenevolution formulas, we found that ≈ 7 per cent of binary HVSs will merge to become, eventually, blue straggler HVSs. Both binary and blue stragglers HVSs have been observed. Edelmann et al. (2005) observed a star moving with a velocity of at least $530\,\mathrm{km\,s^{-1}}$ in the Galactic rest frame. According to stellar atmosphere fits the star is a 9 $M_\odot$ main-sequence star 50 kpc away. The lifetime of this star is several times shorter than its flight time from the MW, suggesting an LMC origin (Gualandris & Portegies Zwart 2007) or a blue straggler origin (Perets 2009). The latter channel suggest that the progenitor was likely a binary system ejected from the MW at $\gtrsim 800\,\mathrm{km\,s^{-1}}$ (Brown 2015). Recently, Németh et al. (2016) have spotted the first binary HVS candidate ≈ 5.7 kpc far from the GC travelling at $\approx 571\,\mathrm{km\,s^{-1}}$.

Brown et al. (2008) showed that HVSs are clustered in the direction of the constellation Leo. Brown, Geller & Kenyon (2012) proposed that the HVS anisotropy could reflect the anisotropy of the Galactic potential. Our model predicts that the anisotropy of HVSs is a natural consequence of cluster motion at the pericentre. This is natural if most stars form in clusters (Kroupa 2005).

Pawlowski, Pflamm-Altenburg & Kroupa (2012) showed that the MW is surrounded by a disc of mostly coorbiting satellite galaxies, the vast polar structure (VPOS) (Kroupa, Theis & Boily 2005). Is the disc of stars around the SMBH of the MW, and/or some gaseous disc there, oriented as the VPOS? The known HVSs do correlate with the VPOS (Pawlowski, Kroupa & Jerjen 2013) and if the innermost accretion disc or circum-nuclear disc of the SMBH is aligned with the VPOS, then results showed in this paper may nicely explain the anisotropy of the flux of HVSs: a moderate embedded cluster forms in the gaseous disc and falls towards the SMBH and produces the HVS flux. This is similar to the dwarf-galaxy picture (Abadi et al. 2009), but is more plausible since stars form in embedded clusters, also in the inner Galaxy, and the youth of the HVSs is then also less of a problem (Brown et al. 2014).

HVSs are powerful tools to investigate the physics of the GC, being in an accessible region of the sky, and also to study the dark sector of our Galaxy (Perets 2009; Fragione & Loeb 2016). When a star cluster passes near the SMBH, it produces HVSs as a consequence of the strong interaction with the SMBH tidal field. If HVSs are generated through the process presented in this paper, by studying their spatial and velocity distribution, it is possible to constrain the physical properties of clusters that have infallen on to the central SMBH, over the course of the MW history, including their binary and mass composition.

REFERENCES

Aarseth S. J., 2003, Gravitational N-body Simulations: Tools and Algorithms. Cambridge Univ. Press, Cambridge

Abadi M. G., Navarro J. F., Steinmetz M., 2009, ApJ, 691, L63

Arca-Sedda M., Capuzzo-Dolcetta R., Spera M., 2016, MNRAS, 456, 2457

Baumgardt H., De Marchi G., Kroupa P., 2008, ApJ, 685, 247

Brown W. R., 2015, ARA&A, 53, 157

Brown W. R., Geller M. J., Kenyon S. J., Kurtz M. J., 2005, ApJ, 622, L33

Brown W. R., Geller M. J., Kenyon S. J., Bromley B. C., 2008, ApJ, 690, L69

Brown W. R., Geller M. J., Kenyon S. J., Diaferio A., 2010, AJ, 139, 59

Brown W. R., Geller M. J., Kenyon S. J., 2012, ApJ, 751, 55

Brown W. R., Geller M. J., Kenyon S. J., 2014, ApJ, 787, 89

Capuzzo-Dolcetta R., Fragione G., 2015, MNRAS, 454, 2677

De Marchi G., Paresce F., Pulone L., 2007, ApJ, 656, L65

Edelmann H., Napiwotzki R., Heber U., Christlieb N., Reimers D., 2005, ApJ, 634, L181

Elmegreen B. G., Shadmehri M., 2003, MNRAS, 338, 817

Fragione G., Capuzzo-Dolcetta R., 2016, MNRAS, 458, 2596

Fragione G., Ginsburg I., 2017, MNRAS, 466, 1805

Fragione G., Loeb A., 2016, preprint (arXiv:1608.01517)

Ginsburg I., Loeb A., 2006, MNRAS, 368, 221

Ginsburg I., Loeb A., 2007, MNRAS, 376, 492

Ginsburg I., Loeb A., Wegner G. A., 2012, MNRAS, 423, 948

Gnedin O. Y., Gould A., Miralda-Escudé J., Zentner A. R., 2005, ApJ, 634, 344

Gnedin O. Y., Brown W. R., Geller M. J., Kenyon S. J., 2010, ApJ, 720, L108

Goodwin S. P., Kroupa P., 2005, A&A, 439, 565

Gould A., Quillen A. C., 2003, ApJ, 592, 935

Gualandris A., Portegies Zwart S., 2007, MNRAS, 376, L29

Haas J., Šubr L., 2016, ApJ, 822, 25

Harfst S., Portegies Zwart S., Stolte A., 2010, MNRAS, 409, 628

Hernquist L., 1990, ApJ, 356, 359

Hills J. G., 1988, Nature, 331, 687

Kenyon S. J., Bromley B. C., Geller M. J., Brown W. R., 2008, ApJ, 680, 312

Kenyon S. J., Bromley B. C., Brown W. R., Geller M. J., 2014, ApJ, 793, 122

King I. R., 1966, AJ, 71, 64

Kroupa P., 1995a, MNRAS, 277, 1491

Kroupa P., 1995b, MNRAS, 277, 1507

Kroupa P., 2001, MNRAS, 322, 231

Kroupa P., 2005, in Turon C., OFlaherty K. S., Perryman M. A. C., eds, ESA SP-576: The Three-Dimensional Universe with Gaia. ESA, Noordwijk, p. 629

Kroupa P., 2008, in Aarseth S. J., Tout C. A., Mardling R. A., eds, Lecture Notes in Physics, Vol. 760, The Cambridge N-Body Lectures. Springer-Verlag, Berlin, p. 181

Kroupa P., Theis C., Boily C. M., 2005, A&A, 431, 517

Kroupa P., Weidner C., Pflamm-Altenburg J., Thies I., Dabringhausen J., Marks M., Maschberger T., 2013, in Oswalt T. D., Gilmore G., eds, Planets, Stars and Stellar Systems. Springer, Netherlands, p. 115

Küpper A. H. W., Maschberger T., Kroupa P., Baumgardt H., 2011, MNRAS, 417, 2300

Leigh N., Umbreit S., Sills A., Knigge C., de Marchi G., Glebbeek E., Sarajedini A., 2012, MNRAS, 422, 1592

Leigh N. W. C., Giersz M., Marks M., Webb J. J., Hypki A., Heinke C. O., Kroupa P., Sills A., 2015, MNRAS, 446, 226

Li Y. et al., 2015, Res. Astron. Astrophys., 15.8, 1364

Löckmann U., Baumgardt H., Kroupa P., 2008, ApJ, 683, L151

Marks M., Kroupa P., 2010, MNRAS, 406, 200

Marks M., Kroupa P., 2012, A&A, 543, A8

Marks M., Kroupa P., Baumgardt H., 2008, MNRAS, 386, 2047

Marks M., Kroupa P., Dabringhausen J., Pawlowski M. S., 2012, MNRAS, 422, 2246

Miyamoto M., Nagai R., 1975, Publ. Astron. Soc. Japan, 27, 533

Navarro J. F., Frenk C. S., White S. D., 1997, ApJ, 490, 493

Németh P., Ziegerer E., Irrgang A., Geier S., Fürst F., Kupfer T., Heber U., 2016, ApJ, 821, L13

O'Leary R. M., Loeb A., 2008, MNRAS, 383, 86

Oh S., Kroupa P., Pflamm-Altenburg J., 2015, ApJ, 805, 92

Pawlowski M. S., Pflamm-Altenburg J., Kroupa P., 2012, MNRAS, 423, 1109

Pawlowski M. S., Kroupa P., Jerjen H., 2013, MNRAS, 435, 1928

Perets H. B., 2009, ApJ, 698, 1330

Perets H. B., Hopman C., Alexander T., 2007, ApJ, 656, 709

Perets H. B., Wu X., Zhao H. S., Famaey B., Gentile G., Alexander T., 2009, ApJ, 697, 2096

Pflamm-Altenburg J., Weidner C., Kroupa P., 2007, ApJ, 671, 1550

Plummer H. C., 1911, MNRAS, 71, 140

Reid M. J. et al., 2014, ApJ, 783, 130

Sana H. et al., 2012, Science, 337, 444

Sari R., Kobayashi S., Rossi E. M., 2010, ApJ, 708, 605

Sesana A., Haardt F., Madau P., 2007, ApJ, 379, L45

Sherwin B., Loeb A., O'Leary R., 2008, MNRAS, 386, 1179

Šubr L., Haas J., 2014, ApJ, 786, 121

Šubr L., Haas J., 2016, ApJ, 828, 1

Tauris T. M., 2015, MNRAS, 448, L6

Weidner C., Kroupa P., 2004, MNRAS, 348, 187

Yu Q., Madau P., 2007, MNRAS, 379, 1293

Yu Q., Tremaine S., 2003, ApJ, 599, 1129

Ziegerer E., Volkert M., Heber U., Irrgang A., Gänsicke B. T., Geier S., 2015, A&A, 576, L14

Zubovas K., Wynn G. A., Gualandris A., 2013, ApJ, 771.2, 118

This paper has been typeset from a TEX/LATEX file prepared by the author.